

Plasma-satellite interaction induced magnetic field perturbations and surface current asymmetry

Saeed ur Rehman and Richard Marchand

Index Terms—Low Earth Orbit, particle sensors, sheath and induced electric effects.

We present the first study of perturbed magnetic fields induced by spacecraft-environment interaction near the recently launched Swarm satellites for selected directions of solar irradiation, as well as for night time conditions. The space environment conditions selected in the analysis correspond to a satellite going over the North magnetic pole, where satellite-induced magnetic field perturbations are expected to be large, and where sudden variations in these perturbations should occur when the satellite crosses the terminator. The induced current density and associated magnetic field perturbations due to the interaction of a Swarm satellite with space plasma are estimated using the particle in cell (PIC) code, PTetra [1]. During day time, the solar illumination considered corresponds to illumination directly from the ram direction (PE in $-X$), the wake direction (PE in X) and Y directions (respectively PE in $+Y$ and PE in $-Y$) in the satellite frame as shown in Fig. 1. The abbreviation PE stands for photo-electron emission. Although the induced current

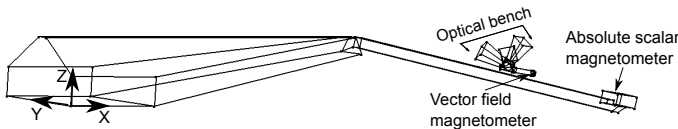


Fig. 1. The simulated Swarm satellite geometry which is 9.2 m in length. Detailed components are omitted from the ram side, but more details are included along the boom, where the vector and scalar magnetometers are located.

densities and magnetic field perturbations are computed for all five cases mentioned above, but they are shown in Fig. 2 only for a case in which sun shine is on the ram direction. This configuration is of interest because of the expected relatively sudden variations in $\delta\vec{B}$ as the satellites cross the terminator. In all simulated cases, the largest perturbed magnetic fields are found to occur near the ram face where induced plasma currents are also the largest. Figure 2 shows the magnitude and selected components of $\delta\vec{B}$ and $\delta\vec{J}$ obtained when solar illumination is on the ram face. Induced currents and perturbed magnetic fields are seen to extend along vertical bands along the background magnetic field. The largest perturbations occur at the ram face, where the induced currents are largest. Weaker perturbations are also visible downstream along the boom, with the largest ones occurring near the optical bench and the scalar magnetometer. It is conspicuous that the spatial structure of magnetic field perturbations found here is qualitatively

S. ur-Rehman and R. Marchand are with the Department of Physics, University of Alberta, Edmonton AB, Canada

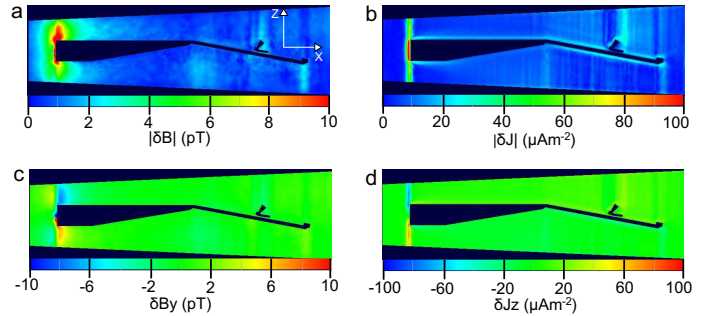


Fig. 2. The perturbed magnetic field (left) and the induced current density (right) are shown in $y = 0$ plane. Panel a shows the absolute value $|\delta\vec{B}|$ and panel c represents the dominant component δB_y . Similarly, right panels (b and d) show the absolute value $|\delta\vec{J}|$ and its dominant component δJ_z .

different from that of electric field perturbations found in the sheath. Indeed except for the wake region, where electric perturbations can extend over distances exceeding the length of a satellite, electric perturbations surrounding a spacecraft tend to be localized near the spacecraft due to Debye shielding [2]. Here, however, induced current densities are not shielded, they extend far from the spacecraft along field lines, and there are no visible perturbations associated with the wake.

The filamentary structure of the perturbed plasma current density and associated perturbed magnetic field can be understood as follows: a) current is mostly carried by electrons, b) in the simulations the unperturbed magnetic field \vec{B} is vertical (along \hat{z}), and c) both thermal and photo-electrons are magnetized and constrained to move along drifting flux tubes of sizes of order one gyro-radius. For the parameters considered, the thermal electron gyro-radius is $\sim 3cm$, while the average photoelectron gyro-radius is $\sim 10cm$. Owing to the relatively small drift velocity compared with the electron thermal velocities of background and photo-electrons ($\sim 1.9 \times 10^5$ and $\sim 7.1 \times 10^5$ respectively), electrons are practically constrained to move along vertical flux tubes. As a consequence, photo-electrons emitted on the ram face, as well as lower energy thermal electrons $\vec{E} \times \vec{B}$ drifting toward the ram face of the satellite and being repelled by the negative spacecraft potential, can only escape along the background magnetic field, thus forming narrow vertical current channels clearly visible in panel d of Fig. 2. Photo-electrons emitted, or thermal electrons approaching the ram face must escape mostly in the $+z$ direction above the spacecraft and in the $-z$ direction below it. This explains the narrow band of negative and positive δJ_z respectively above and below the ram face seen in Fig. 2. The profile of δB_y shown in panel c can be understood from this profile of δJ_z and a straightforward application of Ampère's

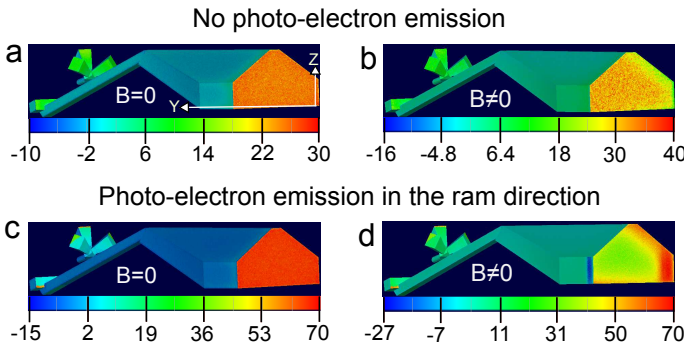


Fig. 3. Computed collected surface current density (μAm^{-2}) at night time (panels a and b) and when solar illumination is from the ram direction (panels c and d) with (panels b and d) and without (panels a and c) the magnetic field.

law. It is important to note that there is no mechanism to shield these field aligned currents at steady state, as would be the case with Debye shielding of electric perturbations. This explains why current filaments extend far from the spacecraft, up to the simulation boundary. These currents would eventually diffuse into the background plasma and close with other current filaments coming from the spacecraft. This closure, however, is not accounted for in the simulations, as it would take place over a much larger volume than is accounted for in the model. In addition to the field perturbations, the asymmetry in the satellite collected surface current are also investigated. Satellites tend to collect positive current on their ram face and negative current in the wake region to ensure a zero net collected current at steady state. For example, Fig. 3 shows the distribution of collected current per unit area with and without a magnetic field at night time and when solar illumination is from the $-X$ direction. As expected, the ram face collects mostly positive current, while negative current is collected on the sides and on the surfaces facing the wake.

With a magnetic field, the ram face collects less positive current as compared to the current collection without magnetic field; this feature is obvious by comparing panels (a) and (b) in Fig. 3. The interpretation is that electrons are magnetized and constrained to a magnetic flux tube of radius of order one electron thermal gyro radius (r_{te}). That is, $r_{te} = v_{te}/\Omega_e$; here v_{te} and Ω_e are the electron thermal velocity and gyro-frequency, respectively. Therefore, relatively less positive current collection is needed on the ram side to compensate the restricted electron current collection mainly on the boom and side surfaces. Due to the convective potential gradient in the satellite frame of reference, the electrostatic sheath potential is stronger on left (in $+y$ direction) side and weaker on right side. Therefore, the left side of the ram face collects more positive current than the right side as obvious in panel (b) of Fig. 3.

In the presence of photo-emission from the ram side, the collected surface currents are more positive on the ram face and more negative on the side surfaces, as apparent in panel (c) of Fig. 3. Note that photo-electron emission contributes to positive collected current, while photo-electron redeposition associated with their relatively short gyro-radius ($\sim 10cm$) contributes to negative current. In the current profile seen in

panel (d) of Fig. 3, the right side of the ram face collects more positive current although the sheath field is weaker there; also, a strip of negative collected current on the left side is noticeable. The emitted photo-electrons from the ram side gyrate clockwise along negative z directed magnetic field lines. The red band to the right of the ram face in panel (d) of Fig. 3 corresponds to the regions where only photo-electrons are emitted from the ram face whereas to the left of that band, both photo-electrons emission and redeposition are occurring thus corresponding to a lower net collected current per unit area on the green band. The blue color strip on the left flank indicates a relatively large negative net collected current per unit area. This is associated with redeposition of photo-electron emitted from the left end of the ram face. It is interesting to note that in this configuration, positive current is collected by part of the optical bench and scalar magnetometer. This is due to photo-emission and the fact that these structures are not completely shadowed by the main spacecraft body. In conclusion, we present the first simulation results leading to quantitative estimates of magnetic field perturbations associated with the interaction between a satellite and its space environment. In the case considered, for Swarm near the North magnetic pole, computed perturbations at the magnetometer locations are found to be well below the instruments' sensitivity threshold, $\sim 50pT$. The sensitive magnetic field measurements made by Swarm will therefore be purely geophysical in origin and no corrections will be needed to account for possible aberrations associated with spacecraft-environment interaction. As the satellites fly over the North pole, however, we predict that under certain conditions, there will be small but systematic variations in the magnetic field associated with satellite-plasma interaction. These variations will occur when the satellites cross the terminator during certain orbit epochs. They will be caused by photoelectrons being turned on and off over a period of approximately 30s. Anticipating future missions to Venus or Mercury in which satellites and instruments would be subject to more intense solar UV radiation, however, it appears that magnetic field perturbations might approach or exceed instruments' sensitivity thresholds.

REFERENCES

[1] R. Marchand, "Ptetra, a tool to simulate low orbit satellite-plasma interaction," *IEEE Trans. Plasma Sci. (USA)*, vol. 40, no. 2, pp. 217 - 29, 2012.
 [2] D. Hastings and H. Garrett, *Spacecraft-Environment Interactions*. Cambridge UK: Cambridge University Press, 2004.